Journal of Applied Polymer Science

Thermosetting Polyurethane-Multiwalled Carbon Nanotube Composites: Thermomechanical Properties and Nanoindentation

Magnovaldo Carvalho Lopes, Vinicius Gomide de Castro, Luciana Moreira Seara, Vitor Perige Almeida Diniz, Rodrigo Lassarote Lavall, Glaura Goulart Silva

Departamento de Química, Instituto de Ciências Exatas, Universidade Federal de Minas Gerais. Av. Pres. Antônio Carlos, 6627, 31270-901 Belo Horizonte—MG, Brazil

Correspondence to: G. G. Silva (e-mail: glaura@qui.ufmg.br or glaurasilva@yahoo.com)

ABSTRACT: In this study, composites based on a thermoset polyurethane elastomer (PU) and multiwalled carbon nanotubes (MWCNT) in the case of a PU of high elastic modulus (>200 MPa) are analyzed for the first time. As-grown and modified nanotubes with 4 wt % of oxygenated functions (MWCNT-ox) were employed to compare their effect on composite properties and maxima mechanical properties (elastic modulus and tensile strength) were reached at 0.5 wt % of MWCNT-ox. Furthermore, by examining the morphology using optical and electron microscopies better dispersion and interaction of the nanotube-matrix was observed for this material. DMTA data supports the observation of an increase in the glass transition temperature of ~20°C in the nanocomposites compared with the thermoset PU, which is an important result because it shows extended reliability in extreme environments. Finally, nanoindentation tests allowed a comparison with the conventional mechanical tests by measuring the elastic modulus and hardness at the subsurface of PU and the nanocomposites. © 2014 Wiley Periodicals, Inc. J. Appl. Polym. Sci. **2014**, *131*, 41207.

KEYWORDS: graphene and fullerenes; mechanical properties; nanotubes; polyurethanes; thermal properties

Received 16 April 2014; accepted 24 June 2014

DOI: 10.1002/app.41207

INTRODUCTION

Materials prepared with carbon nanotubes (CNTs) can outperform conventional materials due to the superior thermal, mechanical and electrical properties of the nanotubes. For example, multiwalled carbon nanotubes (MWCNTs) are electrical conductors, with a Young's modulus ranging from 0.27 to 0.95 TPa and a tensile strength of 11–63 GPa (outermost layer).[1–3] However, due to their high aspect ratio and large amount of van der Waals interactions, CNTs tend to form large aggregates.

The strategy of reinforcing polymers using CNTs has been extensively reviewed[4–6] and has enabled the development of high-performance materials for industrial applications in fields such as aerospace, automotive and sports.[7] The dispersion of the nanotubes in the polymer matrix can be facilitated through the noncovalent or covalent modification of the CNT surface. Covalent modification (functionalization) also enables the formation of a strong nanotube/matrix interface.[4–6] The development of methods to functionalize nanotubes and prepare composites on an industrial scale is considered crucial for achieving innovations.[8]

Polyurethanes (PUs) are available in a large range of chemical structures with extremely versatile properties, exhibiting thermoplastic, elastomeric and thermoset behavior.[9] Among the various types of PUs, thermosetting polyurethane elastomers are frequently used in high-performance products, which demand abrasion resistance, hydrolytic stability, as well as high mechanical and dynamic resistance.[9]

As noted by McClory et al. in 2007[10] and Karabanova et al. in 2013,[11] several polymer composites with carbon nanotubes and thermoplastic polyurethanes were investigated; however, comparatively, there is much less information reported for materials prepared with thermoset PU.[10–13] The first study of a thermoset PU by Xia and Song in 2005[13] presented results for SWCNT and MWCNT composites based on a PU prepared with a polyether polyol and 4,4′-methylenebis(phenyl isocyanate) (MDI) using a dispersion agent and ball milling process. These authors reported improvements in mechanical properties, thermal stability, and thermal conductivity with the carbon nanotube addition.[13] Aided by ultrasound, Xiong et al.[12] prepared composites with an amine modified MWCNT and a concentration of 2 wt % dispersed in a poly(tetramethylene oxide)-based thermoset PU. These authors observed an increase of ~12% in the glass

Additional Supporting Information may be found in the online version of this article.

transition temperature (T_g), an increase in the storage modulus below the T_g, thermal stability and increased mechanical strength compared with the matrix.[12] McClory et al.[10] dispersed MWCNTs in isophorone diisocyanate while employing a high shear mixer; a chain extender was not used in this work. Furthermore, these composites[10] were prepared via a polyether reaction followed by curing at concentrations of 0.1 and 1.0 wt % of nanotubes and resulted in strong enhancements of the mechanical properties.[10] Karabanova et al.[11,14] recently reported a study of a thermoset PU nanocomposite based on poly(oxypropylene)glycol, trimethylol propane and toluene diisocyanate (TDI) by adding MWCNTs (0.01, 0.1, and 0.25 wt %). These authors emphasized the role of the nanotube surface chemistry on the final properties and exploited the differences among nanotubes with acid-oxidation covalently bound and ones with fragments (similar to fulvic acids) only adsorbed to the nanotube surface.[14] A detailed study using dynamic mechanical thermal analysis was performed by these authors,[11] which revealed peculiarities of the glass transition dynamics over a large range of temperatures (~200°C).

In the present work, polymer nanocomposites with neat and acid-treated MWCNTs were prepared by employing a set of techniques that allow for the adequate dispersion of nanotubes and scalable production of nanocomposites. The nanotubes were dispersed in a prepolymer with the aid of a combined high shear disperser and roller mill.[15] Then, the composites were prepared by diluting the masterbatch (nanotube concentration of 5.0 wt %) to achieve contents of 0.25, 0.5, and 1.0 wt %. The effect of the oxygenated covalent modification of the CNT surface and the processing conditions on the dispersion and properties of nanocomposites were evaluated. The PU elastomer employed in this work has a very high modulus (>200 MPa) because it is applied for highly demanding offshore elements, such as kink protectors.[9] It is considered, in general, that the addition of particles for reinforcement could compromise the performance of these high modulus materials, leading to a strong decrease in ductility. Nevertheless, the addition of carbon nanotubes at low concentrations demonstrates where nanotechnology can enhance the material benefits through the addition of very small concentrations, allowing for mechanical reinforcement without compromising other properties. In comparison to the products analyzed here, the literature about thermoset PU/carbon nanotubes all address low moduli PUs, i.e., elastic moduli between 1 and 10 MPa.[10,13,14]

Furthermore, nanoindentation was used to assess the elastic modulus and hardness at the nanoscale subsurface of the PU and nanocomposites for comparison with conventional measurements. This approach has been applied to study polymer–carbon composites, such as the ones based on CNTs or graphene, functionalized or not.[16,17] There are several reports on the use of nanoindentation in epoxy/carbon composites[18–21]; however, few studies have addressed the use of this technique in composites when the matrix is a thermoplastic PU,[17,22,23] and to the best of our knowledge, there is no published work on the mechanical measurements of thermoset PU composites using nanoindentation.

EXPERIMENTAL

Materials

MWCNTs with purity >95%, diameter of 8 nm and length of 30 μm were purchased from Timesnano (China). Two types of nanotubes were employed in this work: as-grown and modified with oxygenated groups (~4% COOH groups according to the supplier), a modified nanotube named MWCNT-ox. The nanotube specifications were verified and will be described in the results section. The prepolymer was kindly provided by the company Plastiprene AS (São Paulo, Brazil), whose formulation contains poly(tetramethylene ether glycol) (PTMG), 2,4-toluene diisocyanate (TDI) (IUPAC name 2,4-diisocyanato-1-methylbenzene) and 1,4-butanediol (IUPAC name Butan-1,4-diol). For the crosslinking reaction, 4,4-methylene-bis-ortho-chloro-aniline (MOCA) (IUPAC name 4-[(4-amino-3-chlorophenyl)methyl]-2-chloroaniline) was used.

The prepolymer synthesis was performed in a stainless steel reactor in an inert atmosphere in the absence of water and at temperatures lower than 100°C to avoid the formation of alophanate and biuret crosslinking. The synthesis occurs in two steps: in the first step, polymerization occurs between the TDI and the PTMG. The molar excess of the TDI in this step guarantees the formation of free isocyanate groups (NCO) at the ends of the prepolymer chains. The second step of the synthesis begins with the addition of 1,4-butanediol (BDO), which acts as a chain extender, increasing the prepolymer molecular weight. The excess of TDI employed resulted in a prepolymer with ~7.5 wt % (determined by titration with dibutylamine) of free NCO.

The content of rigid segments (RSC) in the prepolymer was observed to be ~36% according to eq. (1) [24]:

$$\mathrm{RSC}\,(\%) = [(m_{TDI} + m_{BDO})/(m_{PTMEG} + m_{TDI} + m_{BDO})] \times 100, \quad (1)$$

where m is the mass (in g) of each component of the reaction: TDI, PTMG, and BDO.

Preparation of MWCNT/PU Composites

The goal of the technique employed here for dispersing nanotubes on PU was to process quantities of ~250 g of the masterbatch to attain 1 kg day^{-1} in a pilot production Figure 1. Different methodologies for mixing the CNTs and prepolymer were tested, and the most consistent results were achieved when using a high shear mechanical mixer, a three-roll mill and mechanical agitation as described in the following paragraphs.

For the preparation of the masterbatches Figure 1(a), the prepolymer was heated at 80°C, and MWCNTs (neat and oxygenated) were added at a concentration of 5.0 wt %. For the viscosity tests, a 3.0 wt % concentration of MWCNTs (neat and oxygenated) was used to prepare masterbatches due to the limitations in the range of measures of viscosity of the equipment. Prepolymer heating is essential for reducing viscosity and facilitating nanocomposite processing. Initial homogenization was performed by high shear mixing (vigorous stirring) for a period of 10 min at 24,000 rpm. Afterward, the material was processed repeatedly on a three-roll mill (Exakt) with the rolls heated to 80°C, a rotation of 100 rpm and a 5 μm roller separation.

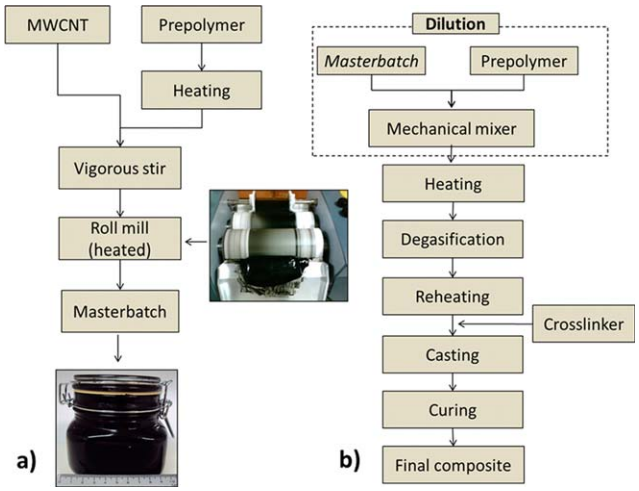

Figure 1. Schematic diagram for the preparation route of PU/MWCNT composites. [Color figure can be viewed in the online issue, which is available at wileyonlinelibrary.com.]

The preparation of the final composite included the diluting the masterbatch [Figure 1(b) dotted part] with the appropriate amount of pure prepolymer to achieve the desired final concentrations (0.25, 0.5, and 1.0 wt %). The dilution process was promoted by mechanical agitation. Next, the PU/MWCNT masterbatch Figure 1(b) was once again heated to 80°C and then held in a vacuum chamber for 15 min to remove air from the material. After deaeration, the dispersion was reheated to 80°C before adding the curing agent (MOCA), which had been oven melted at 110°C. The mass used for the MOCA was proportional to the free —NCO present in the prepolymer. After the addition of MOCA, the mixture was subjected to gentle stirring for ~1 min to prevent bubble formation. Next, the mixture was poured into molds to undergo oven curing at temperatures between 100 and 105°C for a period of 1 h. The nanocomposites were then demolded and subjected to an initial 10-h post-curing process in the oven at 100–105°C. The final post-curing process was performed after 15 days at room temperature. The reheating stages are of great importance because, at a temperature of 25°C, the PU-prepolymer/MWCNT system has a viscosity exceeding 60 Pa s^{-1}. However, at ~80°C, the viscosity is reduced to ~2 Pa s^{-1} to PU and ~5.5 Pa s^{-1} to the composite masterbatches, making processing possible. The viscosity measurements are presented in Figure S1 in the Supporting Information.

Characterization

Thermogravimetric analysis (TGA, Q5000 apparatus, TA instruments) was conducted for the carbonaceous material in a synthetic air atmosphere with a heating rate of 5°C min^{-1} in the temperature range of 20–800°C. The morphology of the MWCNT and MWCNT-ox was analyzed using a scanning electron microscope (SEM) with a cannon emission field effect Quanta 200 - FEG/FEI. The nanotube samples were prepared by sonicating them in isopropyl alcohol and dripping onto silicon substrates. Infrared spectra of the neat and MWCNT-ox were obtained using a FTIR spectrometer (ATR device, model 380 Nicolet Thermo Scientific Smart Performer) with a spectral range of 4000–400 cm^{-1}, a 32 scan acquisition and a resolution of 4 cm^{-1}.

Viscosity data were obtained using a Model DV-III programmable rheometer from Brookfield with a small sample adapter. The viscosity was measured at 25, 70, and 80°C while using a program to increase the rotational speed. Data for comparing the rheological properties of the different dispersions were collected at a shear rate of 0.4 s^{-1} and a 1 rpm rotational speed.

The nanocomposites were characterized by optical microscopy (OM) to observe the distribution of MWCNTs in the polymer matrix. OM was performed with an Olympus microscope (model BX50F) and the morphology of the nanocomposites was also examined by SEM. The nanocomposites were fractured in liquid nitrogen, and their fracture surfaces were coated with a thin layer of gold for SEM analysis. A Tecnai—G2–20/FEI transmission electron microscope (TEM) was used to evaluate the dispersion of the MWCNTs in the PU matrix. The samples were prepared using a cryomicrotomy technique appropriate for TEM measurements.

The mechanical properties of the PU and nanocomposites were evaluated according to the ISO 37 and ASTM D638 standards for testing the modulus and tensile strength at break, respectively. The tests were performed at 22.6°C and a relative humidity of 36.0% using a Kratos model test TRCv59D-USB, a load cell of 100 kgf, and a displacement velocity of 50.0 cm min^{-1}. A minimum of three replicates were performed for each nanocomposite.

Nanocomposite TGA analyses were performed in a synthetic air atmosphere with a heating rate of 10°C min^{-1} for the temperature range from 20 to 800°C using the Q5000 TA instruments apparatus. Infrared spectra of the polyurethane and nanocomposites were obtained using a FTIR spectrometer (ATR device, model 380 Nicolet Thermo Scientific) with a spectral range of 4000–400 cm^{-1}, a 32-scan acquisition and a resolution of 4 cm^{-1}. Dynamic mechanical thermal analysis (DMTA) was performed with TA Instruments Q800. DMTA was performed with a heating rate of 3°C min^{-1}, a temperature range between −150 and 200°C, a 1 Hz frequency and three-point-bending mode. The hardness of the polyurethane and nanocomposites were determined at 23°C and a relative humidity of 57% according to ASTM D 2240 using a Digital Shore D durometer; the final result represents an average of five tests performed for each sample.

The nanoindentation study was performed on a MFP3D nanoindenter (Asylum Research, CA) equipped with a Berkovich diamond indenter tip at room temperature. The PU and nanocomposites were cut into 2 cm × 2 cm × 1 cm samples and glued on stubs. The maximum load was 200 μN, and the loading and unloading rate was 40 μN s^{-1}. To minimize the viscous creep effect, at the maximum load, the indenter was held for 10 s before starting unloading. A total of 36 indentations on a 50 μm × 50 μm area were applied on each sample. The curves were analyzed according to the Oliver–Pharr method,[25] and the average value reported. AFM was performed on the indented areas immediately after the nanoindentation tests.

RESULTS AND DISCUSSION

Characterization of the Carbon Nanotubes

Initially the characteristics reported by the supplier for the MWCNT and MWCNT-ox were verified. The IR spectra in

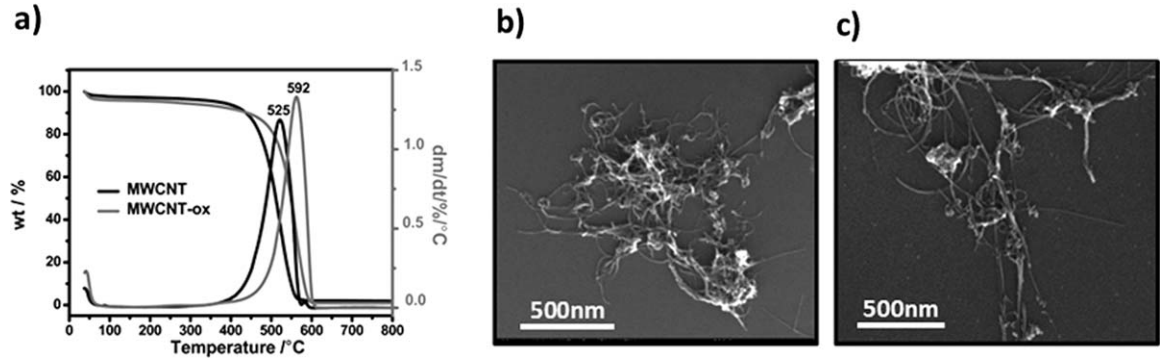

Figure 2. Characterization of neat and oxidized carbon nanotubes: (a) TG and DTG curves and (b), (c) SEM images for MWCNT (b) and MWCNT-ox (c).

Figure S2 in Supporting Information, exhibited a signal at 1580 cm^{-1} that is assigned to C═C stretching in CNTs. The band at 1725 cm^{-1} is ascribed to the C═O stretching of carboxylic acid, which indicates that the functional groups on the modified nanotube surface are carboxyl groups in a large majority, as proposed by the manufacturer.[26,27] Because TGA is an important tool for characterizing the purity and functionalization of CNTs,[28,29] TGA curves and their derivatives (DTG) obtained in synthetic air are presented in Figure 2(a) for MWCNT and MWCNT-ox. The neat nanotube has a high thermal stability at temperatures as high as 400°C, while degradation occurred during a single stage between 400 and 625°C with a mass loss of 93% and a maximum at 525°C (determined on the DTG curve). The TG curves for the MWCNT-ox show a broad and continuous mass loss in the low temperature range (from 120 to 400°C). This event is associated with the loss of functional groups (4 wt %) on the walls of the CNTs[30] and is consistent with the supplier specification. Following this weight loss, nanotube degradation was observed in a single step between 400 and 625°C with a maximum at 592°C and a mass loss of 91%. For both nanotubes, a low residue content (<5%) was observed, thus confirming the purity[28] reported by the manufacturer.

Finally, SEM was used to evaluate the CNT morphology, and images are presented in Figure 2(b,c). The thickness of the nanotubes was confirmed to be ~8 nm, and the length reached several microns, although statistical analysis was not performed. There is no evidence of a difference in the length between the two carbon nanotube samples.

Nanocomposite Characterization

The thermoset PU synthesized in this work was produced by the crosslinking of the prepolymer of PTMG/TDI/BDO with the diamine MOCA (see crosslinking structure in Figure S3 in Supporting Information). For the nanocomposites, after dilution of a prepolymer masterbatch, the crosslinking was conducted *in situ*. The improvement in the polymer properties achieved due to the addition of inorganic nanoparticles is the result of a complex interplay between the interfacial area and interactions. In addition, these factors depend largely on the reinforcement dispersion.[31] The covalent modification of the CNT surface frequently contributes to the optimization of these variables.[32] The range of compositions studied in this work includes the most frequently evaluated concentrations: 0.25, 0.5, and 1.0 wt % of carbon nanotubes.[4–6] The mechanical behavior observed for both nanocomposites, with MWCNT and MWCNT-ox, was consistent with the results observed in Figure 3 for the MWCNT-ox based system. The maxima of the elastic modulus and tensile strength were obtained for the composite with 0.5 wt %.

The behavior of the composites based on the two types of carbon nanotubes is discussed in more detail by comparing the results for the 0.5 wt % nanotube materials. The results of tensile tests, represented by the average of engineering stress × strain curves in Figure 4(a), are summarized in Figure 4(b,c). For nanocomposites prepared with 0.5 wt % MWCNTs, better performance was observed with an average increase of 40 and 47% in the elastic modulus [(Figure 4(b)] with the insertion of as-grown and oxidized nanotubes, respectively. The tensile strength was reduced by an average of 17% with the introduction of neat MWCNTs. However, the tensile strength increased by an average of 32% with the introduction of oxidized MWCNTs [Figure 4(c)]. The strain at break diminished with the addition of neat CNTs; however, a considerable recuperation occurred when oxygenated nanotubes were used [Figure 4(a)], as observed from the average stress versus strain curves.

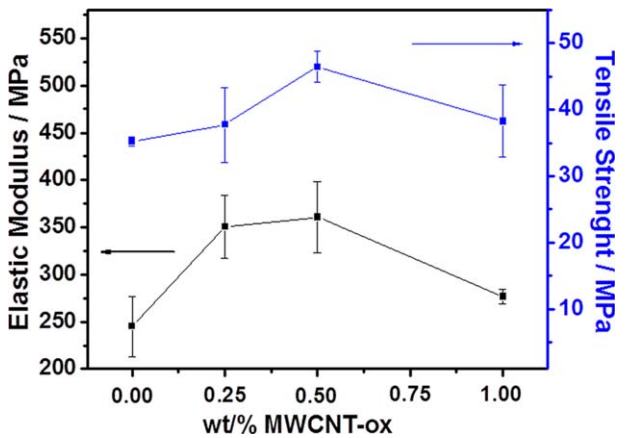

Figure 3. Results of mechanical tests for PU and nanocomposites with MWCNT-ox as a function of nanotube concentration: elastic modulus and tensile strength values. [Color figure can be viewed in the online issue, which is available at wileyonlinelibrary.com.]

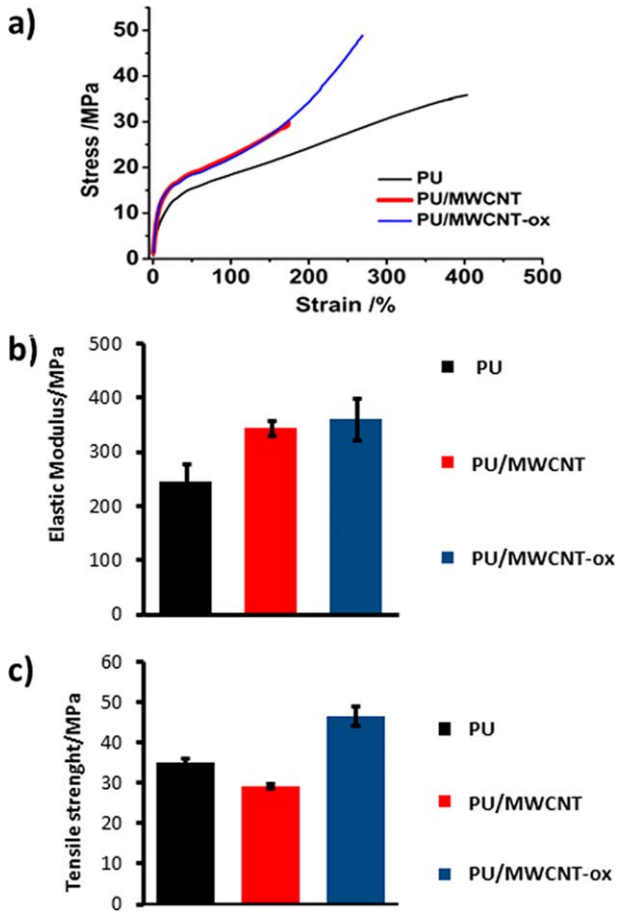

Figure 4. Results of mechanical tests for PU and nanocomposites with 0.5 wt % of neat and oxygenated MWCNTs: (a) engineering stress-strain average curves (from a minimum of three replicates), (b) elastic modulus and (c) tensile strength values. [Color figure can be viewed in the online issue, which is available at wileyonlinelibrary.com.]

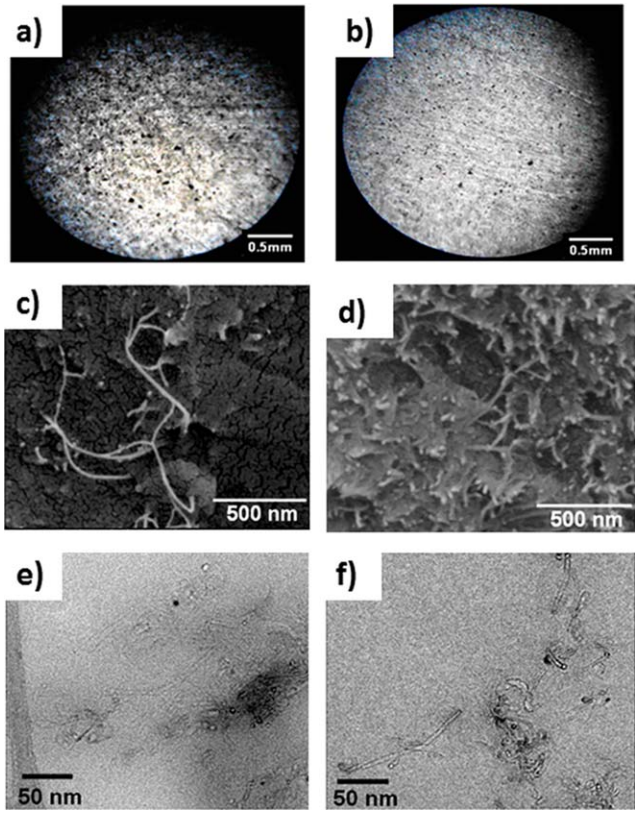

Figure 5. Images of PU-based nanocomposites with 0.5 wt % of nanotubes. Optical microscopy (a,b), SEM (c,d) and TEM (e,f) images for nanocomposites produced with MWCNTs (a,c,e), and MWCNT-ox (b,d,f). [Color figure can be viewed in the online issue, which is available at wileyonlinelibrary.com.]

The mechanical results here can be considered one of the best in relation to similar systems reported in the literature. For instance, Xia and Song[13] prepared polyurethane nanocomposites containing 0.5 wt % of neat carbon and reported a 13% increase in the elastic modulus and a 12% increase in the tensile strength compared with PU. The thermoset polyurethane nanocomposites produced by Xiong et al.[26] exhibited an increase in tensile strength of 63 and 117%, but for large contents of 2 and 5% by mass of CNTs, respectively. As previously stated, the mechanical reinforcement in a nanocomposite is a consequence of the efficient dispersion and interaction between phases. Therefore, it is highly important to study the nanotube dispersion and distribution to interpret the mechanical results. In this context, image analyses at different length scales are fundamental in assessing the dispersion and interfacial features. The OM technique provides a method of evaluating a millimetric film area of the CNT dispersion in the matrix, thus verifying the effectiveness of the different dispersion methods.[32]

Figure 5 presents typical OM images obtained for the composites prepared with unmodified CNTs [Figure 5(a)] and modified CNTs with oxygenated groups [Figure 5(b)] at a concentration of 0.5 wt % nanotubes. The OM comparison between these nanocomposites reveals that the covalently linked oxygenated groups on the CNT surface lead to an improved dispersion because smaller dark aggregates were observed in Figure 5(b). Furthermore, in the SEM images [Figure 5(c,d)], the nanotubes appear to be better covered by the matrix [Figure 5(d)] compared with Figure 5(c), which shows long, detached portions of nanotubes. Our results are similar to the SEM images of fractured composite surfaces with thermosetting PU acquired by Xiong et al.[12] This group was able to examine an exposed surface of functionalized CNTs coated by the matrix, and their results indicate good compatibility between the PU and nanotubes.[12] Nevertheless, it is important to note that both SEM images presented in Figures 5(c,d) do not exhibit any evidence that the CNTs have been pulled out of the matrix during the fracture process. This result supports the conclusion of a presence of good adhesion in the nanotube-matrix in both cases, which is a necessity for efficient mechanical reinforcement. Typical TEM images of the cryomicrotomic composite are presented in Figures 5(e,f). The TEM analysis further demonstrates that the dispersion of the modified CNTs was improved compared with the neat CNTs [Figure 5(f)]. The images can be used to confirm that the improved adhesion between the nanotube-matrix enabled the effective transfer of stress during a mechanical process, as observed in the mechanical results.

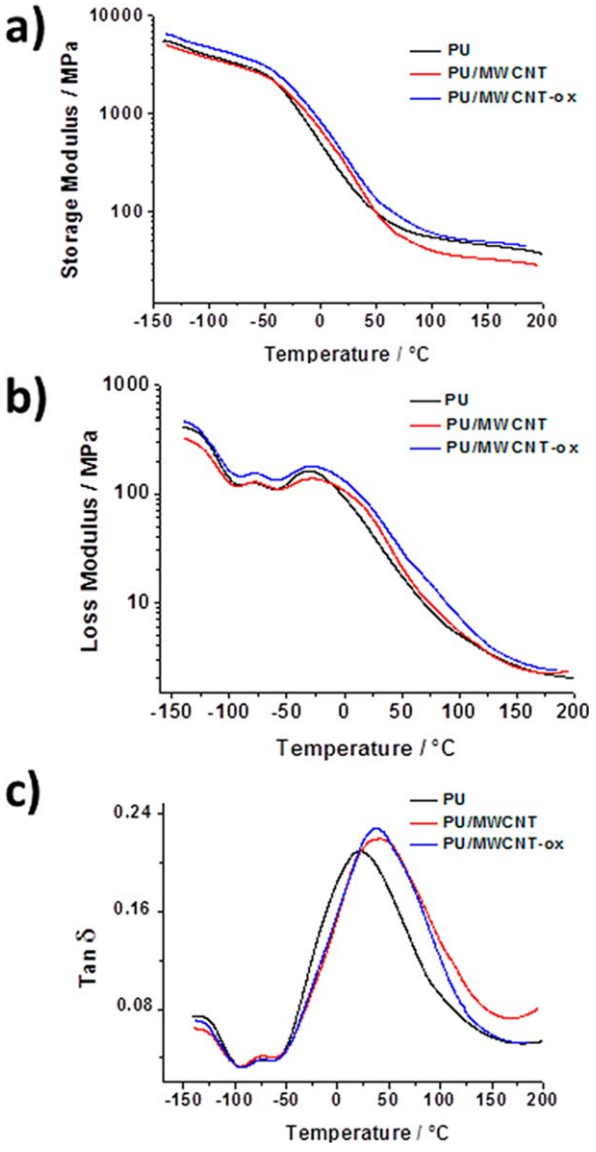

Figure 6. Dynamic mechanical thermal analysis (DMTA) for PU and nanocomposites with 0.5 wt % of MWCNTs and MWCNT-ox: (a) storage modulus, (b) loss modulus and (c) tan δ curves. [Color figure can be viewed in the online issue, which is available at wileyonlinelibrary.com.]

Moreover, the study of the glass transition temperature (T_g) can provide important information concerning the interactions between nanoparticles and the composite polymer matrix. For instance, T_g can vary substantially with respect to the polymer in nanocomposites. T_g can decrease when the polymer–nanoparticle interface has free surfaces ("non-wet" interfaces with low adhesion) and increase when the interface forms strong interfaces due to the attractive interactions between the components.[31] In particular, the T_g of crosslinked polymeric systems is associated with the degree of the resin cure. Therefore, the interplay between the reinforcement effect of the particles and their possible disruptive effect on the polymer chain crosslinking is important for tailoring the material.[33]

Xiong et al.[12] previously described the preparation of thermosetting PU nanocomposites with a concentration of 5 wt % of

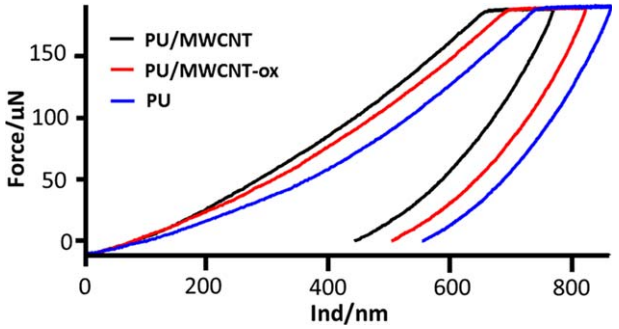

Figure 7. Example of load versus displacement indentation curves for PU and nanocomposite samples produced with 0.5 wt % of MWCNTs and MWCNT-ox. [Color figure can be viewed in the online issue, which is available at wileyonlinelibrary.com.]

nanotubes and a T_g increase of ~20°C compared with PU. The same group also reported the preparation of a different PU thermoset nanocomposite containing 2 wt % of CNTs and a T_g increase of 12°C.[12] An increase in the T_g of a thermoset polyurethane nanocomposite was also reported by McClory et al.[10] This group was able to achieve a T_g increase of 10°C for nanocomposites with 1 wt % of CNTs.

The DMTA results for PU and nanocomposites with 0.5 wt % of carbon nanotubes are presented in Figure 6. The storage modulus [Figure 6(a)] is slightly high for the PU/MWCNT-ox at low temperatures, below 75°C, compared with the neat thermoset PU. The tan δ curves contain a very large peak for all the samples, indicating that there was considerable overlap between the thermal transitions associated with the hard and soft domains in this thermoset PU. This behavior is similar to that observed by Karabanova et al.[11] with a thermoset based on poly(oxypropylene glycol)/TDI and trimethylolpropane. At least two overlapping peaks are present in the tan δ spectra [Figure 6(c)] for all the samples, which can be separated into two glass transitions, presumably for the soft domains (−50–75°C) and hard domains (0–150°C). This pronounced heterogeneity of the domains undergoing the glass transition led to the extremely broad peak in tan δ; however, its maxima can be considered as a reference for the hard domain T_g.

The increase in the T_g of the hard domains (as the maxima in the tan δ peak) for nanocomposites with 0.5 wt % of CNTs compared with PU (an increase of ~20°C) can be observed in Figure 6(c). This increase in T_g was observed in this case while using a CNT mass 10 times lower than that previously reported for thermoset PU nanocomposites.[26] This increase in T_g clearly demonstrates that the CNTs affect the macromolecular structure, therefore leading to a material with lower chain mobility. The CNT network reinforcement in the composite can be considered as the main reason behind the decrease in segment flexibility. Furthermore, we can affirm that the CNTs did not disturb the crosslinking reaction.

Seeking evidence regarding the change in the chemical structure of the nanocomposites compared with the PU structure, infrared spectra were obtained and are presented in Figure S4 in Supporting Information. The conclusion of the detailed analysis performed in these spectra for all the important bands is that it

Table I. Nanoindentation Data—Hardness (H) and Young's Modulus (E) for PU and Nanocomposites with 0.5 wt % of CNTs

Sample	H (MPa)	E (MPa)	h_{max} (nm)[a]	h_{res}[a]/h_{max}	E/H
PU	18.7 ± 2.0	176.1 ± 13.9	840.8 ± 37.7	0.77	9.4
PU/MWCNT	23.7 ± 1.8	211.5 ± 8.7	753.7 ± 19.4	0.76	8.9
PU/MWCNT-ox	19.1 ± 1.0	186.9 ± 5.9	820.7 ± 17.1	0.78	9.8

[a] h_{max} = displacement at maximum load; h_{res} = residual displacement after load removal.

is not possible to observe any significant change in the position or intensity of the signals. This result may be a consequence of the low content of nanotubes and the overlap of important contributions for the bands, such as the ones associated with symmetric stretching of the N—H hydrogen bond at 3280 cm^{-1}; symmetrical stretching of C=O at 1695 cm^{-1}; symmetrical stretching of urethane C—N at 1220 cm^{-1}; and bending of polyether C—O—C at 1101 cm^{-1}. Therefore, it is not possible to propose a preferential interaction of the CNTs to flexible or rigid domains in the present work, which may also be associated with the low degree of phase separation between the domains in this type of thermoset.

Finally, nanoindentation was used to complete the characterization of the materials with the goal of obtaining subsurface data (indentation of ~800 nm) to compare with the conventional mechanical tests. Figure 7 presents typical indentation curves for PU and the nanocomposite samples with 0.5 wt % of MWCNTs and MWCNT-ox. The load *versus* displacement curves were used to calculate the Young's modulus (E) and hardness (H) according to the Oliver–Pharr method.[25] The average values for these properties are listed in Table I. A few minutes after indentation occurred on the surface, the samples recovered completely, making it impossible to capture images of the indent marks using AFM.

The elastic moduli measured by nanoindentation were also in the range of 200 MPa, even though the values were smaller than the ones obtained by conventional mechanical tensile testing. Table I demonstrates that the addition of 0.5 wt % of MWCNTs to the PU matrix has a significant effect on the hardness and elastic modulus values. Improvements of 27% in the hardness and 20% in the elastic modulus were observed. The enhancement in modulus is equivalent to half that obtained in the conventional mechanical test. The addition of MWCNT-ox also improved the mechanical properties of the PU from the nanoindentation viewpoint but not as much as the non-functionalized MWCNTs. These results differ from those observed in the conventional mechanical tests in Figure 4, where better properties were observed with the oxygenated nanotubes. The maximum displacement (h_{max}) under the maximum load for the PU/MWCNT composite decreases as observed for other indentation loads in previous tests not shown here. Table I also lists the calculated parameter (h_{res}/h_{max}), which is the ratio between the residual depth and the maximum depth observed in the test. This parameter can range from 0 (fully elastic behavior) to 1 (behavior of a rigid plastic).[22] The values of this ratio for the three samples were ~0.8, nearest to hard plastic, showing that the thermoset polyurethane was very stiff. Complementary Shore D hardness measurements were performed, and the results showed the same tendency as the conventional mechanical tests; the MWCNT-ox led to a higher improvement in this parameter, although the values were not very different: 57, 58, and 59 Shore D for the PU, MWCNT nanocomposites and MWCNT-ox nanocomposites, respectively.

One possible explanation for the better mechanical performance observed in the nanoindentation test for the MWCNT-based composite, as opposed to the MWCNT-ox one, is the difference in the enrichment at the sub-surface region with the reinforcement; the MWCNTs, which have a less compatible interaction with the matrix, may be more available at the sub-surface. However, this hypothesis must be verified in the future.

CONCLUSIONS

In this study, improvements in the mechanical and thermal properties of PU/CNT composites have been observed: T_g increased by 20°C, and the elastic modulus increased by 47% after adding a small amount of MWCNT-ox to the nanocomposites (0.5 wt %). Furthermore, the oxidized nanotubes are better dispersed in the matrix, as characterized by optical and electron microscopies. Nevertheless, the nanoindentation test showed a higher gain in elastic modulus (20%) for the nanocomposite with MWCNTs than for the modified nanotube-based composite. This finding may be associated with the differences in the distribution of the reinforcement being richer at the sub-surface of the samples for the non-modified CNTs.

ACKNOWLEDGMENTS

The authors thank the Petrobras Company for support. They thank Daniel Freller of Plastiprene, a Brazilian producer of polyurethane parts, the Pró-Reitoria de Pesquisa of UFMG and the Microscopic Center (UFMG).

REFERENCES

1. Kim, P.; Shi, L.; Majumdar, A.; McEuen, P. L. *Phys. Rev. Lett.* **2001**, *87*, 215502.
2. Yu, M.-F.; Lourie, O.; Dyer, M. J.; Moloni, K.; Kelly, T. F.; Ruoff, R. S. *Science* **2000**, *287*, 637.
3. Yang, D. J.; Wang, S. G.; Zhang, Q.; Sellin, P. J.; Chen, G. *Phys. Lett. A.* **2004**, *329*, 207.
4. Spitalsky, Z.; Tasis, D.; Papagelis, K.; Galiotis, C. *Prog. Polym. Sci.* **2010**, *35*, 357.
5. Bose, S.; Khare, R. A.; Moldenaers, P. *Polymer* **2010**, *51*, 975.
6. Sahoo, N. G.; Rana, S.; Cho, J. W.; Li, L.; Chan, S. H. *Prog. Polym. Sci.* **2010**, *35*, 837.

7. Jorio, A.; Dresselhaus, G.; Dresselhaus, M. S. Carbon Nanotubes—Advanced Topics in the Synthesis, Structure, Properties and Applications; Springer: Berlin, **2008**; Vol. *111*, Chapter 2, p 13.
8. De Volder, M. F. L.; Tawfick, S. H.; Baughman, R. H.; Hart, A. J. *Science* **2013**, *339*, 535.
9. Hans-Wilhelm, E.; Hans-Georg, P.; Reinhard, A.; Rolf, W. A.; Jens, K.; Andreas, H.; Holger, C.; Jeff, D. *ChemInform.* **2013**, *36*, 9422.
10. McClory, C.; McNally, T.; Brennan, G. P.; Erskine, J. *J. Appl. Polym. Sci.* **2007**, *105*, 1003.
11. Karabanova, L.; Whitby, R. D.; Bershtein, V.; Korobeinyk, A.; Yakushev, P.; Bondaruk, O.; Lloyd, A.; Mikhalovsky, S. *Colloid Polym. Sci.* **2013**, *291*, 573.
12. Xiong, J.; Zheng, Z.; Qin, X.; Li, M.; Li, H.; Wang, X. *Carbon* **2006**, *44*, 2701.
13. Xia, H.; Song, M. *Soft Matter.* **2005**, *1*, 386.
14. Karabanova, L. V.; Whitby, R. L. D.; Korobeinyk, A.; Bondaruk, O.; Salvage, J. P.; Lloyd, A. W.; Mikhalovsky, S. V. *Compos. Sci. Technol.* **2012**, *72*, 865.
15. Ma, P.-C.; Siddiqui, N. A.; Marom, G.; Kim, J.-K. *Compos. A Appl. Sci. Manufact.* **2010**, *41*, 1345.
16. Rahman, R. *J. Appl. Phys.* **2013**, *113*, 243503.
17. Cai, D.; Jin, J.; Yusoh, K.; Rafiq, R.; Song, M. *Compos. Sci. Technol.* **2012**, *72*, 702.
18. Lee, H.; Mall, S.; He, P.; Shi, D.; Narasimhadevara, S.; Yun, Y.-H.; Shanov, V.; Schulz, M. J. *Compos. B Eng.* **2007**, *38*, 58.
19. Li, X.-F.; Lau, K.-T.; Yin, Y.-S. *Compos. Sci. Technol.* **2008**, *68*, 2876.
20. Ribeiro, H.; Silva, W.; Rodrigues, M.-T.; Neves, J.; Paniago, R.; Fantini, C.; Calado, H. D. R.; Seara, L. M.; Silva, G. G. *J. Mater. Sci.* **2013**, *48*, 7883.
21. King, J. A.; Klimek, D. R.; Miskioglu, I.; Odegard, G. M. *J. Appl. Polym. Sci.* **2013**, *128*, 4217.
22. Gupta, T. K.; Singh, B. P.; Dhakate, S. R.; Singh, V. N.; Mathur, R. B. *J. Mater. Chem. A* **2013**, *1*, 9138.
23. Fulcher, J. T.; Lu, Y. C.; Tandon, G. P.; Foster, D. C. *Polym. Test.* **2010**, *29*, 544.
24. Korley, L. T. J.; Pate, B. D.; Thomas, E. L.; Hammond, P. T. *Polymer* **2006**, *47*, 3073.
25. Oliver, W. C.; Pharr, G. M. *J. Mater. Res.* **1992**, *7*, 1564.
26. Xiong, J.; Zheng, Z.; Song, W.; Zhou, D.; Wang, X. *Compos. A Appl. Sci. Manufact.* **2008**, *39*, 904.
27. Zhao, C.; Ji, L.; Liu, H.; Hu, G.; Zhang, S.; Yang, M.; Yang, Z. *J. Solid State Chem.* **2004**, *177*, 4394.
28. Trigueiro, J. P. C.; Silva, G. G.; Lavall, R. L.; Furtado, C. A.; Oliveira, S.; Ferlauto, A. S.; Lacerda, R. G.; Ladeira, L. O.; Liu, J.-W.; Frost, R. L.; George, G. A. J. *Nanosci. Nanotechnol.* **2007**, *7*, 3477.
29. Musumeci, A. W.; Silva, G. G.; Martens, W. N.; Waclawik, E. R.; Frost, R. L. *J. Therm. Anal. Calorim.* **2007**, *88*, 885.
30. Wang, T.-L.; Yu, C.-C.; Yang, C.-H.; Shieh, Y.-T.; Tsai, Y.-Z.; Wang, N.-F. *J. Nanomater.* **2011**, *2011*, 1.
31. Perla, R.; Rodney, D. P.; Linda, J. B.; John, M. T. *Nat. Mater.* **2007**, *6*, 278.
32. Jung, Y. C.; Yoo, H. J.; Kim, Y. A.; Cho, J. W.; Endo, M. *Carbon* **2010**, *48*, 1598.
33. Putz, K. W.; Palmeri, M. J.; Cohn, R. B.; Andrews, R.; Brinson, L. C. *Macromolecules* **2008**, *41*, 6752.